Journal of Alloys and Compounds 509 (2011) 2176–2179

Contents lists available at ScienceDirect

Journal of Alloys and Compounds

journal homepage: www.elsevier.com/locate/jallcom

Effect of Ag film thickness on the optical and the electrical properties in $CuAlO_2$/Ag/$CuAlO_2$ multilayer films grown on glass substrates

Dohyun Oh[a,b], Young Soo No[a], Su Youn Kim[a], Woon Jo Cho[b], Kae Dal Kwack[a], Tae Whan Kim[a,*]

[a] Department of Electronics and Computer Engineering, Hanyang University, 17 Haengdang-dong, Seongdong-gu, Seoul 133-791, Republic of Korea
[b] Nano Convergence Device Center, Korea Institute of Science and Technology, Seoul 136-791, Republic of Korea

ARTICLE INFO

Article history:
Received 3 July 2010
Received in revised form 26 October 2010
Accepted 28 October 2010
Available online 9 November 2010

PACS:
68.65.Ac
72.15.Eb
73.21.Ac
78.66.Bz

Keywords:
Oxide materials
Thin films
Electronic properties
Optical properties
Atomic force microscopy
AFM
X-ray diffraction

ABSTRACT

Effects of Ag film thickness on the optical and the electrical properties in $CuAlO_2$/Ag/$CuAlO_2$ multilayer films grown on glass substrates were investigated. Atomic force microscopy images showed that Ag films with a thickness of a few nanometers had island structures. X-ray diffraction patterns showed that the phase of the $CuAlO_2$ layer was amorphous. The resistivity of the 40 nm-$CuAlO_2$/18 nm-Ag/40 nm-$CuAlO_2$ multilayer films was 2.8×10^{-5} Ω cm, and the transmittance of the multilayer films with an Ag film thickness of 8 nm was approximately 89.16%. These results indicate that $CuAlO_2$/Ag/$CuAlO_2$ multilayer films grown on glass substrates hold promise for potential applications as transparent conducting electrodes in high-efficiency solar cells.

1. Introduction

Transparent conducting oxide (TCO) films have attracted a great deal of interest for potential applications as transparent electrodes in electronic and optoelectronic devices due to their excellent electrical and optical properties. The efficiency and performance of devices in promising applications, such as solar cells, organic light-emitting diodes (OLEDs), and photodetectors, are significantly affected by the electrical and the optical properties of the TCO films [1–3]. The prospect of potential applications of next-generation electronic and optoelectronic devices utilizing TCO films has led to substantial research and development efforts to form TCO films that act as a window layer for light transmission, photocurrent generation, and current collection in thin film photovoltaic technologies [4,5]. Among the various kinds of TCO films, ZnO:Al, In_2O_3:Sn, SnO_2:F, and TiO_2:Nb have been the most extensively studied n-type semiconductors [6–9]. However, relatively little work has been done on p-type TCO films [10]. Rapid advancements in p-type TCO $CuAlO_2$ film growth technologies utilizing p- and n-type TCO films have made possible the fabrication of transparent optoelectronic devices, such as solar cells, OLEDs, and photodetectors [11–14].

However, because the conductivity of $CuAlO_2$ films is 3 orders of magnitude smaller than commonly used n-type TCO, the improvement of the electrical property of $CuAlO_2$ films is essential for applications in practical devices. Metal-based transparent conductor films with a sandwich multilayer have been suggested to achieve low electric resistance and excellent transmittance in the visible region [15–19]. Very thin metal film is used to improve the electrical conductivity, and semiconductor or dielectric layers deposited on both sides of the metal film suppress reflection from the metal in the visible region, resulting in an enhancement of the selective transparent effect. Even though some studies concerning the formation and the physical properties of the multilayer films consisting of a very thin metal layer sandwiched between dielectric layers have been conducted [15–22], very few studies on the electrical and optical properties of $CuAlO_2$/Ag/$CuAlO_2$ multilayer films grown on glass substrates have been performed.

This paper reports data for the effect of Ag thickness on the optical and the electrical properties of $CuAlO_2$/Ag/$CuAlO_2$ multilayer films grown on glass substrates using a radio-frequency

* Corresponding author. Tel.: +82 2 2220 0354; fax: +82 2 2292 4135.
E-mail address: twk@hanyang.ac.kr (T.W. Kim).

0925-8388/$ – see front matter © 2010 Elsevier B.V. All rights reserved.
doi:10.1016/j.jallcom.2010.10.180

magnetron sputtering method. The thicknesses of the Ag thin films were varied to enhance the optical and the electrical properties of $CuAlO_2$/Ag/$CuAlO_2$ multilayer films with low resistivity and high transmission. Atomic force microscopy (AFM) and X-ray diffraction (XRD) measurements were performed to investigate the surface and the structural properties of the $CuAlO_2$/Ag/$CuAlO_2$ multilayer films, and Hall effect measurements were carried out to determine their resistivity. Transmittance measurements were performed to investigate the optical properties of the films.

2. Experimental details

$CuAlO_2$/Ag/$CuAlO_2$ multilayer films with various Ag thicknesses were prepared on glass substrates using a tilted dual target RF magnetron sputtering system at room temperature. The $CuAlO_2$ target was prepared using the solid-state reaction of the stoichiometry mixture of Cu_2O and Al_2O_3 powder in a furnace at 1200 °C for 24 h. The substrates were degreased in trichloroethylene (TCE), rinsed in de-ionized water, etched in a mixture of HF and H_2O (1:1) at room temperature for 5 min, and rinsed in TCE again. After the glass substrates were cleaned chemically, they were mounted onto a holder in a deposition chamber. After the chamber was evacuated to 2×10^{-6} Torr, the deposition was done at a room temperature. Ar gas with a purity of 99.9999% was used as the sputtering gas, and the flow rate of the Ar gas for the growth of $CuAlO_2$/Ag/$CuAlO_2$ multilayer films is 10 SCCM. Prior to $CuAlO_2$/Ag/$CuAlO_2$ multilayer film growth, the surfaces of the $CuAlO_2$ and the Ag target were polished using Ar^+ pre-sputtering. The $CuAlO_2$ and Ag depositions were done on a glass substrate at a system pressure of 0.005 Torr and a radio-frequency (RF) power (RF = 13.26 MHz) of 100 W. The distance between the substrate and the targets was 7 cm. The multilayer films were deposited continuously without breaking the vacuum at room temperature.

The AFM measurements were performed using XE-100 atomic force microscopy. The XRD measurements were performed using a Rigaku D/Max-B diffractometer with Cu Kα radiation. The Hall effect measurements were performed using a four-point probe. The optical transmittance measurements were performed with a UV–vis spectrophotometer in the wavelength range of 300–800 nm.

3. Results and discussion

The thickness of the upper and lower $CuAlO_2$ layers was fixed to 40 nm to investigate the effect of Ag film thickness on the surface, optical, and electrical properties of $CuAlO_2$/Ag/$CuAlO_2$ multilayer films. Fig. 1 shows the XRD patterns for the $CuAlO_2$/Ag/$CuAlO_2$ multilayer films grown on glass substrates at different Ag film thicknesses. XRD patterns showed that the (1 1 1) diffraction peak at 37.9° corresponding to the Ag films is clearly observed, indicating that the as-grown Ag films have a single crystal phase. The broad peak around 24.5° is related to the glass substrate. The XRD patterns for the $CuAlO_2$/Ag/$CuAlO_2$ multilayer films indicate that the intensity of the Ag (1 1 1) peak increases with increasing thickness of Ag film from 2 to 18 nm. There was no XRD peak corresponding to the $CuAlO_2$ layer observed, indicating that the as-grown $CuAlO_2$ films have an amorphous phase. Therefore, the multilayer films containing a single crystalline Ag film and amorphous $CuAlO_2$ layers are formed on glass substrates.

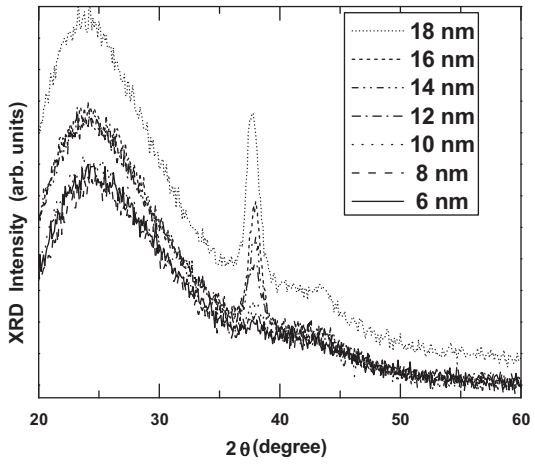

Fig. 1. X-ray diffraction patterns for the $CuAlO_2$/Ag/$CuAlO_2$ multilayer films grown on glass substrates with different Ag film thicknesses.

Fig. 2 shows the AFM images for the (a) $CuAlO_2$ film with a thickness of 40 nm and the Ag films with thicknesses of (b) 2, (c) 4, (d) 6, and (e) 8 nm. After the $CuAlO_2$ film was deposited on the glass substrate, Ag films were deposited on the $CuAlO_2$ coated glass sub-

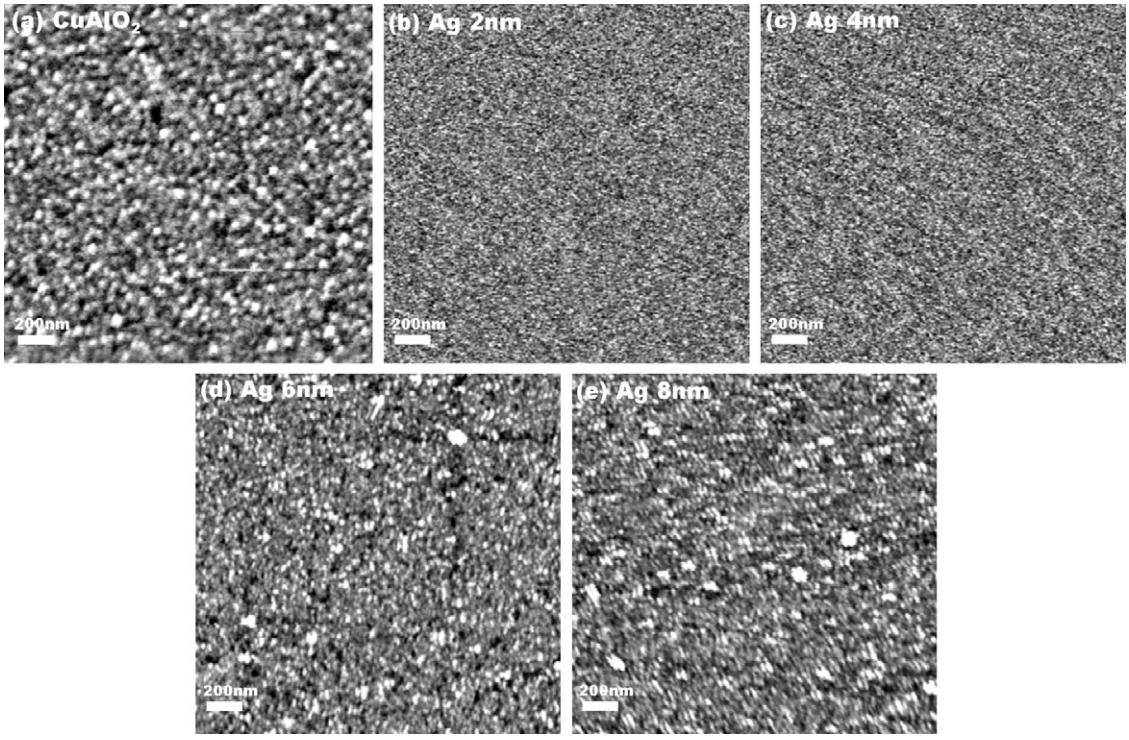

Fig. 2. Atomic force microscopy images for the (a) $CuAlO_2$ film with a thickness of 40 nm and the Ag films with thicknesses of (b) 2, (c) 4, (d) 6, and (e) 8 nm.

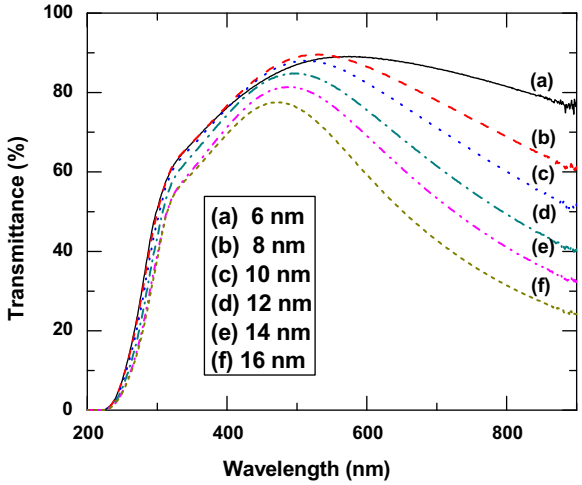

Fig. 3. Optical transmittance spectra observed for the $CuAlO_2$/Ag/$CuAlO_2$ multilayer films with different Ag films thicknesses of (a) 6, (b) 8, (c) 10, (d) 12, (e) 14, and (f) 16 nm.

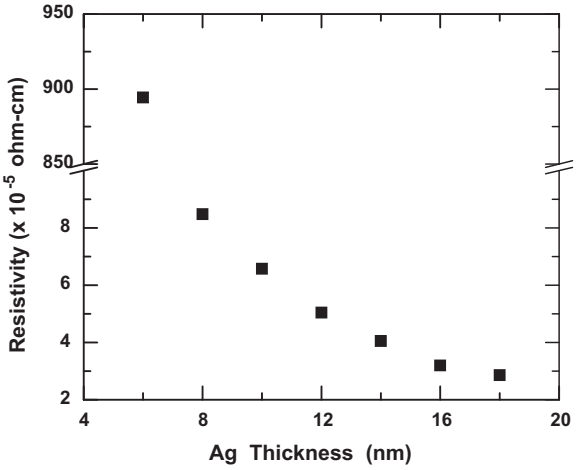

Fig. 4. Resistivity as a function of the Ag film thickness for the $CuAlO_2$/Ag/$CuAlO_2$ multilayer films.

strate. The morphology of the $CuAlO_2$ film deposited on the glass substrate showed a uniform surface with a root mean square (RMS) value of 0.5 nm, as shown in Fig. 2(a). The morphology of the Ag film with a thickness of 2 nm exhibits a discrete island rather than a continuous property, as shown in Fig. 2(b). The morphology of the Ag film with a thickness of 4 nm is similar to that of Ag film with a thickness of 2 nm, as shown in Fig. 2(c). The surface of the Ag film with a thickness of 6 nm contains irregular holes, as shown in Fig. 2(d). The morphology of the Ag film with a thickness of 8 nm exhibits a homogeneous surface, as shown in Fig. 2(e). The homogeneous morphology of the Ag film inserted between the $CuAlO_2$ films significantly affects the optical and the electrical properties of the $CuAlO_2$ films on glass substrates. An Ag film with a thickness of 8 nm with a homogeneous surface increases the transmission of the $CuAlO_2$/Ag/$CuAlO_2$ multilayer film, and the Ag film can decrease the resistivity of the $CuAlO_2$/Ag/$CuAlO_2$ multilayer film.

Fig. 3 shows the transmittance spectra for the $CuAlO_2$/Ag/$CuAlO_2$ multilayer films with different Ag film thicknesses in the wavelength range between 200 and 900 nm. While the transmittance of the multilayer films increases with an increase in the thickness of the Ag film from 6 to 8 nm, their transmittance decreases with increasing Ag film thickness above 8 nm. The transmittance peak with a maximum intensity for the $CuAlO_2$/Ag/$CuAlO_2$ films appears at an approximately 550 nm wavelength, regardless of the Ag film thickness. The maximum transmission of the $CuAlO_2$/Ag/$CuAlO_2$ films as a function of the Ag film thickness is shown in Fig. 3(b). The maximum transmission for the $CuAlO_2$/Ag/$CuAlO_2$ multilayer film with an Ag film thickness of 8 nm is approximately 89.16%. The increase of the transmission for the $CuAlO_2$/Ag/$CuAlO_2$ multilayer film with an Ag film thickness of 8 nm originates from the homogeneous surface of the inserted Ag film. The optical transmittances of the $CuAlO_2$/Ag/$CuAlO_2$ multilayer films in the visible wavelength region significantly depend on the thicknesses of the Ag layer.

Fig. 4 shows the resistivity as a function of the Ag film thickness for the $CuAlO_2$/Ag/$CuAlO_2$ multilayer films. The resistivity decreases with increasing Ag film thickness. The morphology of the Ag film for the $CuAlO_2$/Ag/$CuAlO_2$ multilayer film with an Ag film thickness of 6 nm has irregular and discrete pores, as shown in Fig. 2(d), resulting in an increase of resistivity. The resistivity of the $CuAlO_2$/Ag/$CuAlO_2$ multilayer film with an Ag film above the film thickness of 8 nm significantly decreases with increasing Ag film thickness. The dramatic decrease of the resistivity for the $CuAlO_2$/Ag/$CuAlO_2$ multilayer film with an Ag film above the film thickness of 8 nm might be attributed to the homogeneous surface of the embedded Ag film and to the increase of the Ag film thickness. The resistivity of the $CuAlO_2$/Ag/$CuAlO_2$ multilayer film with an Ag film thickness of 18 nm is as low as approximately $2.8 \times 10^{-5}\ \Omega$ cm, which is much smaller than the resistivity of the conventional ITO film.

The resistivity variations of the $CuAlO_2$/Ag/$CuAlO_2$ multilayer films with an Ag thickness of 10 nm annealed at different annealing temperatures in an oxygen atmosphere are shown in Fig. 5. The resistivity decreases with increasing annealing temperature from 100 to 350 °C. The lowest resistivity of $4.05 \times 10^{-5}\ \Omega$ cm for the $CuAlO_2$/Ag/$CuAlO_2$ multilayer films was obtained at an annealing temperature of 350 °C because the crystallinities and the heterointerface qualities of the $CuAlO_2$/Ag/$CuAlO_2$ multilayer films were improved with increasing annealing temperature.

4. Summary and conclusions

The $CuAlO_2$/Ag/$CuAlO_2$ multilayer films were grown on glass substrates using radio-frequency magnetron sputtering at room temperature. The morphology of the Ag films with a thickness of 8 nm was uniform. The morphology of the Ag films inserted in the $CuAlO_2$ films significantly affected the optical transmit-

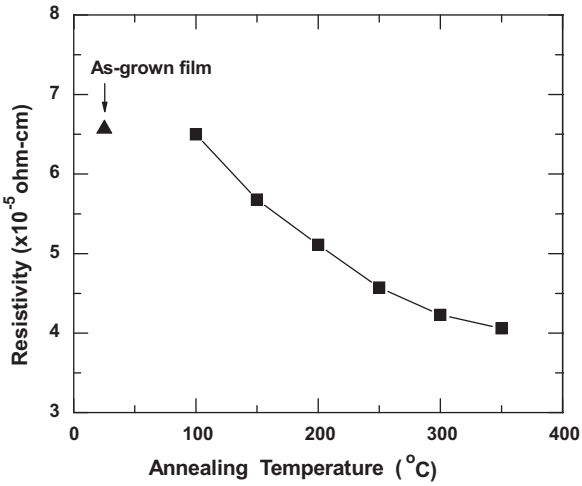

Fig. 5. Resistivity variations of the $CuAlO_2$/Ag/$CuAlO_2$ multilayer films with an Ag thickness of 10 nm annealed at different annealing temperatures in an oxygen atmosphere.

tance and the resistivity of the $CuAlO_2$/Ag/$CuAlO_2$ multilayer films deposited on glass substrates. The maximum transmittance of the $CuAlO_2$/Ag/$CuAlO_2$ multilayer films with a thickness of 8 nm was 89.16%. The resistivity of the $CuAlO_2$/Ag/$CuAlO_2$ multilayer films with an Ag film thickness of 18 nm was as small as about $2.8 \times 10^{-5}\ \Omega$ cm. The resistivity of the $CuAlO_2$/Ag/$CuAlO_2$ multilayer films was decreased as a result of the thermal annealing treatment. These results indicate that $CuAlO_2$/Ag/$CuAlO_2$ multilayer films grown on glass substrates hold promise for potential applications as TCO films in solar cells.

Acknowledgement

This work was supported by the Korea Research Foundation Grant funded by the Korean Government (MOEHRD, Basic Research Promotion Fund) (KRF-2006-005-J04102).

References

[1] D. Song, A.G. Aberle, J. Xia, Appl. Surf. Sci. 195 (2002) 291–296.
[2] T. Schuler, M.A. Aegerter, Thin Solid Films 351 (1999) 125–131.
[3] K. Matsubara, P. Fons, K. Iwata, A. Yamada, K. Sakurai, H. Tampo, S. Niki, Thin Solid Films 431 (2003) 369–372.
[4] J. Muller, B. Rech, J. Springer, M. Vanecek, Sol. Energy 77 (2004) 917–930.
[5] J. Elias, R. Tena-Zaera, C. Levy-Clement, Thin Solid Films 515 (2007) 8553–8557.
[6] K. Ip, Y.W. Heo, K.H. Baik, D.P. Norton, S.J. Pearton, F. Ren, Appl. Phys. Lett. 84 (2004) 544–546.
[7] S.H. Kim, N.M. Park, T.Y. Kim, G.Y. Sung, Thin Solid Films 475 (2005) 262–266.
[8] T.W. Kim, D.C. Choo, Y.S. No, W.K. Choi, E.H. Choi, Appl. Surf. Sci. 253 (2006) 1917–1920.
[9] C.M. Maghanga, J. Jensen, G.A. Niklasson, C.G. Granqvist, M. Mwamburi, Sol. Energy Mater. Sol. Cells 94 (2010) 75–79.
[10] H. Kawazoe, M. Yasukawa, H. Hyodo, M. Kurita, H. Yanagi, H. Hosono, Nature 389 (1997) 939–942.
[11] H. Ohta, M. Hirano, K. Nakahara, H. Maruta, T. Tanabe, M. Kamiya, T. Kamiya, H. Hosono, Appl. Phys. Lett. 83 (2003) 1029–1031.
[12] H. Ohta, T. Kambayashi, M. Hirano, H. Hoshi, K. Ishikawa, H. Takezoe, H. Hosono, Adv. Mater. 15 (2003) 1258–1262.
[13] H. Ohta, T. Kambayashi, K. Nomura, M. Hirano, K. Ishikawa, H. Takezoe, H. Hosono, Adv. Mater. 16 (2004) 312–316.
[14] A.N. Banerjee, S. Nandy, C.K. Ghosh, K.K. Chattopadhyay, Thin Solid Films 515 (2007) 7324–7330.
[15] E. Ando, M. Miyazaki, Thin Solid Films 516 (2008) 4574–4577.
[16] M. Fahland, T. Vogt, W. Schoenberger, N. Schiller, Thin Solid Films 516 (2008) 5777–5780.
[17] D.R. Sahu, S.-Y. Lin, J.-L. Huang, Thin Solid Films 516 (2008) 4728–4732.
[18] J.-A. Jeong, Y.-S. Park, H.-K. Kim, J. Appl. Phys. 107 (2010) 023111-1–023111-8.
[19] S. Song, T. Yang, Y. Xin, L. Jiang, Y. Li, Z. Pang, M. Lv, S. Han, Curr. Appl. Phys. 10 (2010) 452–456.
[20] Y.S. Kim, J.H. Park, D.H. Choi, H.S. Jang, J.H. Lee, H.J. Park, J.I. Choi, D.H. Ju, J.Y. Lee, D. Kim, Appl. Surf. Sci. 254 (2007) 1524–1527.
[21] C.-H. Cheng, J.-M. Ting, Thin Solid Films 516 (2007) 203–207.
[22] J.-A. Jeong, H.-K. Kim, M.-S. Yi, Appl. Phys. Lett. 93 (2008) 033301-1–033301-3.